07

Registration of pulsed terahertz radiation with uncooled matrix microbolometric detectors

© M.A. Dem'yanenko,[1] I.V. Marchishin,[1] D.V. Sheglov,[1] V.V. Startsev[2]

[1] Rzhanov Institute of Semiconductor Physics, Siberian Branch, Russian Academy of Sciences, 630090 Novosibirsk, Russia
[2] Joint-Stock Company Scientific and Production Association„Orion"(JSC „SPA „Orion", 111538 Moscow, Russia
e-mail: demyanenko@isp.nsc.ru

Received April 9, 2024
Revised June 11, 2024
Accepted June 18, 2024

The response of uncooled matrix microbolometric detectors with a thin metal absorber to pulsed terahertz radiation is studied depending on the pulse duration, its repetition frequency, thermal conductivity and bolometer thermal relaxation time, which change with increasing gas pressure in the receiver housing, as well as on the polarization of terahertz radiation. It is shown that the peak value of the microbolometer signal weakly depends on thermal conductivity if the duration of the radiation pulses is less than the bolometer thermal relaxation time. Under the opposite condition, the peak value of the microbolometer signal is inversely proportional to the thermal conductivity value. The manufactured and investigated detectors at a wavelength of 100 μm are characterized by a minimum detectable power of $1.4 \cdot 10^{-9}$ W and a minimum detectable energy of $2.5 \cdot 10^{-11}$ J.

Keywords: Thermal conductivity, thermal relaxation time, minimum detectable energy.

DOI: 10.61011/TP.2024.08.59016.115-24

Introduction

Uncooled matrix microbolometer detectors are (MMBD) traditionally applied in the systems of registration of infrared (IR) [1,2] and terahertz (THz) radiation [3–9] with constant or slowly varying intensity, i.e. when characteristic time of variation of radiation power that falls on the detector is considerably higher than the time of thermal relaxation of bolometers. However, in a series of cases application of pulsed radiation enables improvement of the accuracy of measurement as a result of elimination of constant or low-frequency parasitic signals and noise. For instance, a differential method using pulsed THz radiation was applied already in one of the first studies of registration of THz radiation with matrix microbolometers which allows for the subtraction of a constant parasitic signal from background IR radiation and for the reduction of $1/f$ noise [4]. In some cases, such as registration of THz radiation reflected from a remote object, including the generation of the image of the object, highlighting by powerful radiation is required due to scattering [10] and a significant absorption in the atmosphere [11]. In such cases a short duration pulsed radiation can be applied to reduce energy costs and improve the safety just as it is applied for atmosphere remote sensing [12–17], remote detection of toxic [18,19] or radioactive [20,21] substances. The use of pulsed THz radiation may be also attributable to the fact that some of the radiation sources, for instance, radiation sources based on photoconductive antennas [22,23] and nonlinear optical crystals [24] have a pulsed mode of operation, or, like quantum cascade lasers (QCL) [25–27], they have a considerably higher power in the pulsed mode of operation. Since the advent of systems designed to emit high-power picosecond pulses of THz radiation at a repetition frequency of 1 Hz to 1 kHz with an energy of a single pulse from 0.4 to 55 mJ [28–31], and microsecond pulses with energies up to 1 J [32,33], it has become possible to create high-speed pulse systems of registration of THz images, operating in snapshot mode [34], including the operation in several spectral subranges, for example, selected by additional filters. In particular, a single pulse of THz radiation with an energy of 1 mJ allows (without taking into account absorption and scattering losses) obtaining a terahertz image in 10 spectral subranges of equal energy with signal-to-noise ratio of ≈ 1300 on matrix detectors with size of 320×240 that have minimum detectable energy of $1 \cdot 10^{-12}$ J, which can be easily verified by a simple calculation ($320 \times 240 \times 10^{-12} \times 1300 \approx 10^{-3}/10$).

For the successful application of uncooled microbolometer detectors in various applications and studies that require registration of pulsed THz radiation, it is necessary not only to increase the sensitivity and speed, but it is also necessary to study their operation in the pulsed illumination mode. A fairly general analytical equations for the temperature response of the bolometer to periodic radiation pulses was obtained in Ref. [34]. It was theoretically shown and experimentally confirmed on the example of IR bolometers that the bolometers with high thermal conductivity and accordingly reduced thermal relaxation time, despite the reduced sensitivity to continuous radiation, can be highly efficient for registration of radiation pulses with a duration less than the bolometer thermal relaxation time. It was

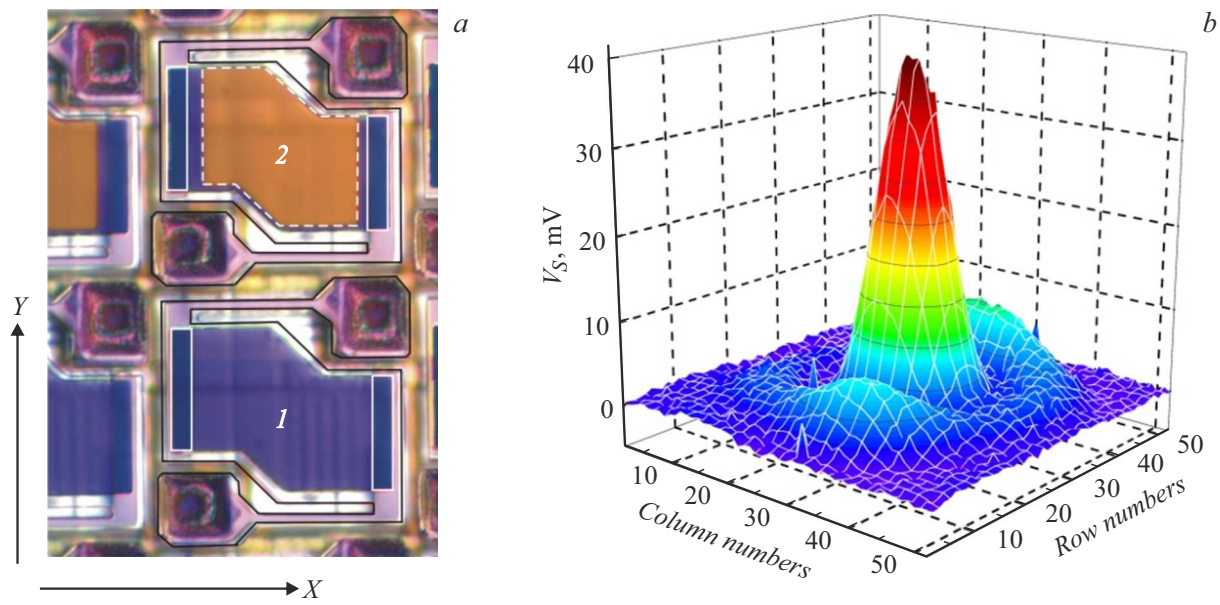

Figure 1. *a* — MMBD fragment: *1* — microbolometer without metal absorber, *2* — with absorber (highlighted in white dotted line); *b* — distribution of signal peak value V_S along the rows and columns of the MMBD when it is illuminated by pulsed THz radiation (wavelength of 100 μm, pulse frequency 7 Hz, pulse ratio 2). Radiation falls on the MMBD region containing only microbolometers with a metal absorber. The pressure in the MMBD housing is $2.5 \cdot 10^{-5}$ mbar.

also shown there that uncooled matrix detectors of pulsed terahertz radiation, characterized by a minimum detectable energy of less than $1 \cdot 10^{-12}$ J, and frame rate up to 1000 Hz can be developed based on such bolometers.

The dependences of the magnitude of terahertz signal of an uncooled MMBD with a thin metal absorber on the magnitude of the thermal conductivity and the bolometer thermal relaxation time, radiation pulse duration, pulse repetition frequency and the direction of polarization of terahertz radiation are experimentally studied in this paper. Comparison with the theoretical ratios given in Ref. [34] are provided.

1. Experimental procedure

Experimental studies are conducted using MMBD with the format of 320×240 pixels manufactured by Institute of Semiconductor Physics of Siberian Branch of the Russian Academy of Sciences (Novosibirsk) and a 100 μm quantum cascade laser (TeraCascade 100 QCL, Lytid SAS). MMBD pixels with size $51 \times 51\,\mu$m consist of microbolometers, each of which is a thermosensitive membrane suspended on thin, weakly thermally conductive beams above a silicon substrate with a signal reading circuitry. The thermosensitive membrane consists of two ≈ 150 nm thick layers of silicon oxynitride, acting as carrier and passivation layers, and a ≈ 100 nm thick vanadium oxide layer, grown by reactive ion-beam method and acting as a thermosensitive resistance. The suspension height of the bolometer membrane above the silicon substrate is $\approx 2\,\mu$m and is close to the optimal value, which ensures the effective absorption of IR radiation with wavelengths of the order of 10 μm. More detailed description of the MMBD, including description of the principle of operation of the silicon readout circuit, can be found in Ref. [35,36]. The MMBD studied in this paper differed from detectors presented in Ref. [35,36] designed for the spectral range of $8-14\,\mu$m in the use of a thin metal radiation absorber with a close to optimal layer resistance $\approx 70\,\Omega/\square$ [5.37] that was applied to the membrane of the microbolometers of the first 182 rows of the matrix detector for increasing the absorption coefficient of THz-radiation; the bolometers of the remaining 58 rows did not have the metal absorber (Fig. 1, *a*). Also, unlike studies in Ref. [6,35,36], in which the germanium input window with an anti-reflective coating that increases transmission in the range of $8-14\,\mu$m was applied in the MMBD vacuum casing, in the present work, the input window with a thickness of 2 mm was made of anti-reflective coated, high resistance silicon, more transparent in the THz region [37].

Signals from MMBD elements were read line-by-line at a frame rate of 25 or 50 Hz, so that the elements of each subsequent line were measured 40 ms/240 $\approx 166\,\mu$s or 20 ms/240 $\approx 83\,\mu$s after the measurement of the preceding line. THz radiation was modulated either at different frequencies (from 3 to 511 Hz) with a pulse ratio of 2 using hardware built into the QCL, or with a short external pulse voltage synchronized with the frame pulse controlling the operation of the MMBD, while the pulse ratio could reach 20. The thermal conductivity of the bolometer G_0 and the thermal relaxation time of the bolometer τ_0 were $0.8 \cdot 10^{-7}$ W/K and 15 ms respectively at high vacuum. After pumping the MMBD vacuum housing

to $2.5 \cdot 10^{-5}$ mbar, the turbomolecular vacuum pump was switched off, and the gas pressure in the housing gradually increased, which resulted in an increase of the bolometer thermal conductivity G and a decrease of the bolometer thermal relaxation time $\tau = C/G$, where C is the heat capacity of the bolometer which is equal to $\sim 1.2 \cdot 10^{-9}$ J/K. The direction of polarization of THz radiation relative to microbolometers was changed by rotating the MMBD vacuum housing around the axis of the tube through which air was pumped out of the MMBD housing.

2. Response of microbolometric detectors to pulsed THz radiation with low pulse ratio

Figure 1, *b* shows 3*D*-topogram of the peak (maximum in time) value of the MMBD response (signal) V_S illuminated by a THz radiation pulse with duration of $t_p \approx 70$ ms, at which the time dependence of the signal reached saturation (since t_p significantly exceeds $\tau_0 = 15$ ms) and, therefore, the peak signal was equal to the signal in continuous illumination mode. QCL and MMBD were not synchronized in these measurements: the repetition period of radiation pulses Θ was ~ 140 ms and was significantly higher than the time of recording of a single frame (40 ms). Consequently, the measured values of signals can vary from a maximum (peak) values (if the signal was read from illuminated lines at the time of saturation of the signal) to zero (if the signal was read from illuminated lines before the arrival of the next pulse), therefore, the frame with the maximum signal value V_S was selected from a series of sequentially measured frames for determining the peak signal value. The QCL radiation was focused using a polymethylpentene (PMP) or TPX lens on the MMBD area containing only a microbolometer with a metal absorber. Main part of the radiation was concentrated in a spot with the size of 20×20 pixels. The power P_{THz} of QCL radiation incident on the MMBD was determined using pyroelectric detector THZ5I-BL-BNC (Gentec Electro-Optics, Inc.) and was $\sim 50\,\mu$W. The integral value of the signal V_S for all pixels exposed to radiation $V_{S,\mathrm{Int}}$ was $8.7 \cdot 10^3$ mV. The sensitivity of microbolometers to „constant" THz radiation $S = V_{S,\mathrm{Int}}/P_{\mathrm{THz}}$ was $\sim 1.8 \cdot 10^5$ V/W, which gives the minimum detectable power of $P_{\mathrm{th}} = V_{\mathrm{noise}}/S = 1.4 \cdot 10^{-9}$ W taking into account the magnitude of the noise of the detector of $V_{\mathrm{noise}} = 0.25$ mV. The power of radiation incident on the pixel corresponding to the maximum signal of $V_{S,\max} \approx 41$ mV (Fig. 1, *b*) is determined by the ratio of $P_{\mathrm{pix,max}} = V_{S,\max}/S$ and amounts to $\sim 2.3 \cdot 10^{-7}$ W.

There are additional lobes in the form of a ring around the main peak of the distribution of MMBD signals (Fig. 1, *b*). The value of the signal on the ring has an angular dependence with a significant decrease of the signal along the line passing through the maximum of the main peak. The number of rings increased (up to 10 and more) as the radiation defocused with a simultaneous decrease of the value of the main maximum. Such a distribution of the QCL registered radiation in the form of concentric rings is attributable to the interference of the radiation emerging from its two end faces located at a distance of about 1 mm [38,39]. Furthermore, the lens, the output window of QCL and the input window of MMBD can make an additional contribution to the interference.

The QCL radiation was focused on the boundary of the MMBD regions containing microbolometers with and without a metal absorber for studying the effect of a thin metal absorber on the magnitude of the detector signal. The direction of polarization of THz radiation was either vertical (along the axis Y in Fig. 1, *a*) or horizontal (along the axis X in Fig. 1, *a*). Fig. 2 shows the results of measurements performed using QCL modulation with a frequency of 50 Hz (pulse ratio equal to 2). It is clear that thin metal absorber increases the value of the bolometer signal V_S in case of the vertical polarization of the THz radiation by more than two times. The value of the signal is much less for horizontal polarization in the presence of the absorber than for vertical polarization (by about 5 times), and the signal is almost absent ($V_S \approx 1$ mV) in the absence of the absorber. Such polarization dependence of the signal can be explained by the fact that, a quite effective absorption of vertically polarized THz radiation in the absence of the absorber is attributable to the vertically spaced contacts to the heat-sensitive layer of vanadium oxide (highlighted by white solid lines in Fig. 1, *a*), performing the role of micro antennae (width of $4\,\mu$m, length of $24\,\mu$m, layer resistance of $\approx 10\,\Omega/\square$, which ensures the longitudinal resistance equal to $60\,\Omega$, which is close to the characteristic radiation resistance of half wave dipole antenna). The horizontally arranged busbars (width $1.5-2\,\mu$m, length $30\,\mu$mm, layer resistance $\approx 25\,\Omega/\square$) running along the supporting beams of the microbolometer have a longitudinal resistance $\approx 375-500\,\Omega$, which is much larger than the characteristic radiation resistance of a half-wave dipole antenna, and are therefore inefficient radiation absorbers for both polarizations.

The above-mentioned strong dependence of the magnitude of the MMBD signal V_S on the direction of polarization of THz radiation indicates that the mechanism of its formation differs from that in the spectral range of $8-14\,\mu$m, in which virtually no polarization dependence is observed. This can also cause doubt in bolometric nature of the measured signal, based on the fact that the radiation heats the temperature-sensitive membrane and accordingly the temperature-sensitive resistance. An alternative signal conditioning mechanism, given the much lower emission frequencies, could be, for example, a rectification mechanism at the $p-n$-junctions of the silicon readout circuitry of microantenna-induced alternating voltage. This provided additional incentive for performing the following studies which found a good agreement of the experimental dependences of the signal value on the THz-radiation pulse duration, its repetition frequency, and the gas pressure in the MMBD housing with the calculations performed

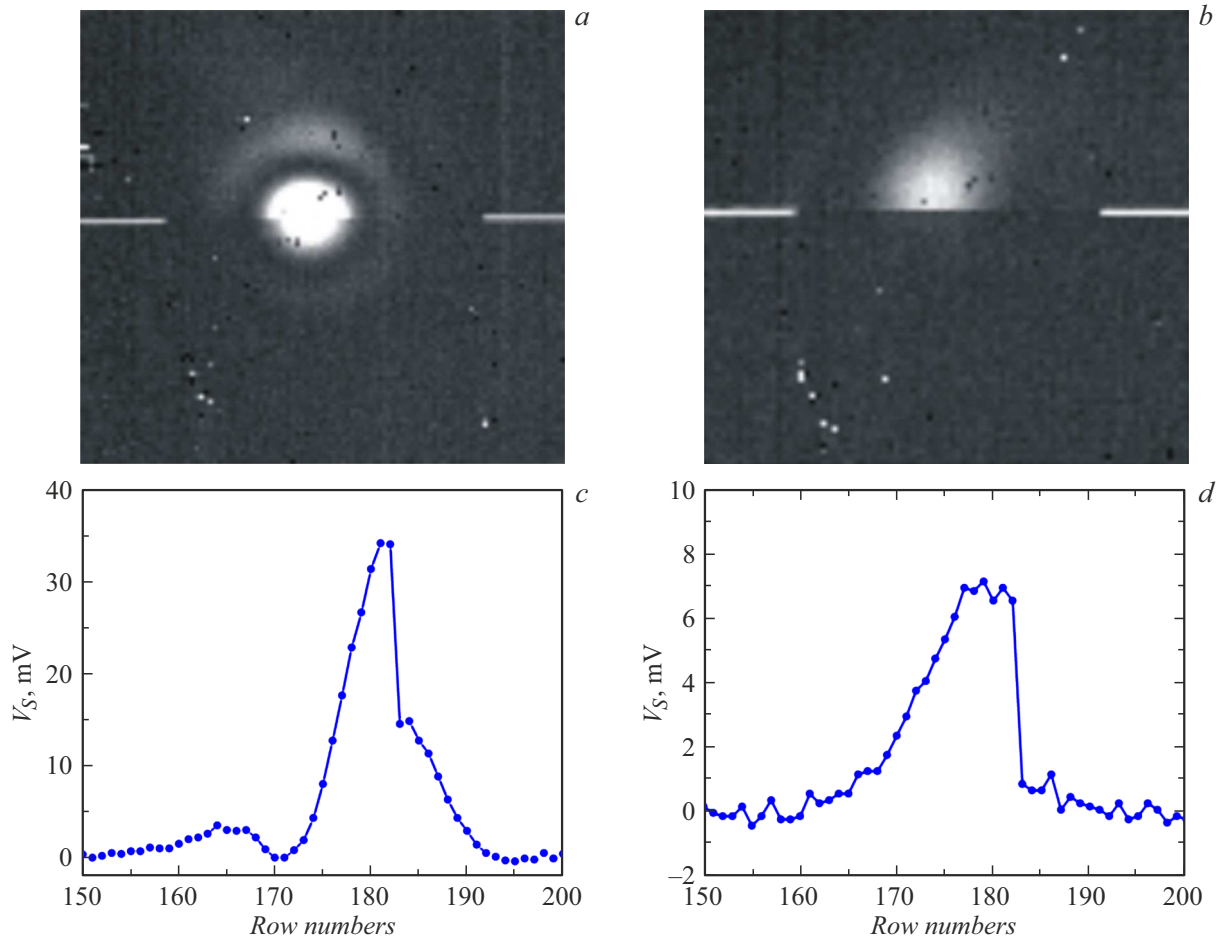

Figure 2. Topograms of signals of the MMBB illuminated by pulsed by pulsed THz radiation with a wavelength of 100 μm (a, b) and of distribution of the signal over the sensitive elements of the column passing through the maximum of the signal (c, d). The boundary of the MMBD regions containing microbolometers with and without a metal absorber lies between lines 182 and 183 (it is marked with white horizontal dashes in a, b). The polarization of THz radiation is vertical (along the axis Y in Figure 1, a) (a, c) and horizontal (along the axis X in Figure 1, a) (b, d). The pressure in the MMBD housing is $2.5 \cdot 10^{-5}$ mbar.

within the bolometric model which confidently confirms the bolometric nature of the signal.

The effect of radiation pulse repetition rate was studied by focusing the QCL radiation onto the MMBD region containing only microbolometers with a thin metal absorber and by varying the pulse frequency f from 3 to 511 Hz at a constant pulse rate equal to 2. Given the unsynchronized mode of operation of QCL and MMBD, as well as a large range of THz radiation pulse repetition rates, including frequencies both much lower and much higher than the frame frequency of the detector, equal to 25 Hz, the mean value of the signal $V_{S,\text{mean}}$ and its RMS deviation from the mean value $V_{S,\text{rms}}$, which were calculated over 50 consecutively measured frames, were chosen as the measured values. 3D-topogram of RMS deviation $V_{S,\text{rms}}$measured with a pulse repetition rate of 7 Hz, is shown in Fig. 3, a. The topogram of the mean value of the signal $V_{S,\text{mean}}$ had a similar form, but its value was a little higher. The frequency dependences of $V_{S,\text{mean}}$ and $V_{S,\text{rms}}$ shown in Fig. 3, b were measured on pixels corresponding to the maximum values of $V_{S,\text{mean}}$ on the 3D-topogram. Average value of $V_{S,\text{mean}}$ virtually does not depend on the pulse repetition rate of the THz radiation, and the RMS deviation $V_{S,\text{rms}}$ is close to the average at frequencies of less than 5 Hz and decreases inversely proportional to the frequency f when its value is greater than 20 Hz.

The above behavior of $V_{S,\text{mean}}$ and $V_{S,\text{rms}}$ can be explained by the dependence of the response of the bolometer V_S on the time t when it is exposed to the rectangular radiation pulses following with different frequencies (Fig. 4), calculated using the relations given in [34]. Due to the symmetry of the bolometer response relative to the value $V_{S,P\text{mean}}$, caused by the constant radiation with power P_{mean}, equal to the time-average value of the power of the modulated radiation incident on the bolometer, available at the pulse ratio of 2, the mean value of the signal $V_{S,\text{mean}}$ turns out to be equal to $V_{S,P\text{mean}}$ and does not depend on the pulse frequency. In this case, the value $V_{S,\text{mean}}$ is equal to half of the maximum value of $V_{S,\text{max}}$ achieved in case of illumination by radiation pulses with the duration

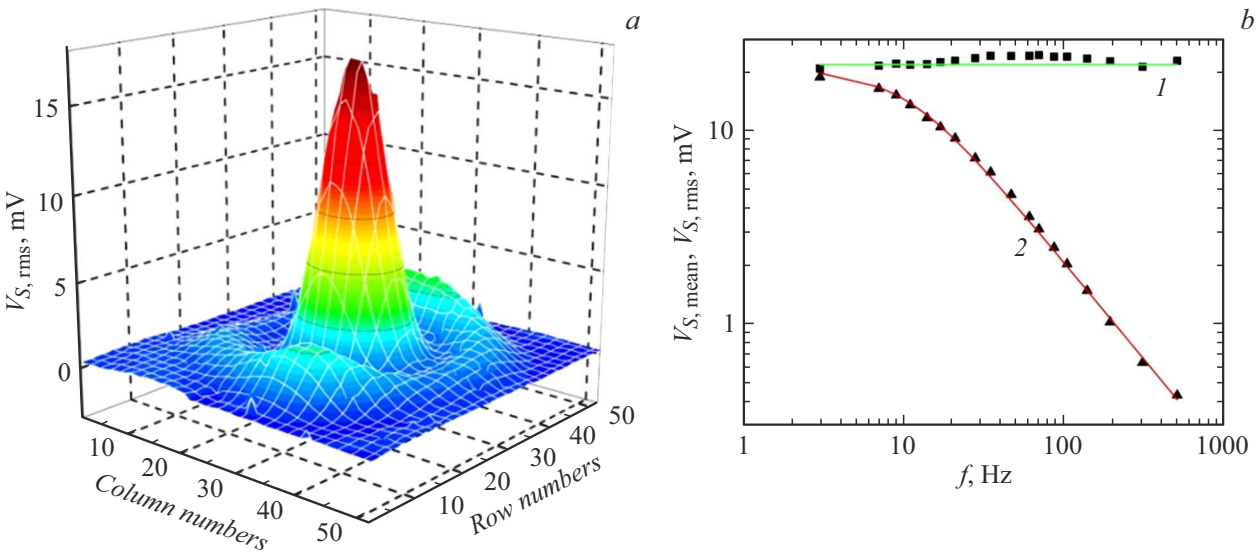

Figure 3. *a* — 3*D*-topogram of the RMS deviation of signal $V_{S,\mathrm{rms}}$ of the MMBD illuminated by pulsed THz radiation (wavelength 100 μm, pulse frequency 7 Hz, pulse ratio 2); *b* dependences of the maximum values of the average signal $V_{S,\mathrm{mean}}$ (curve *1*) and its RMS deviation $V_{S,\mathrm{rms}}$ (curve *2*) on the THz pulse repetition rate f. The experiment data are shown by dots, calculated data are shown by lines. The pressure in the MMBD housing is $2.5 \cdot 10^{-5}$ mbar.

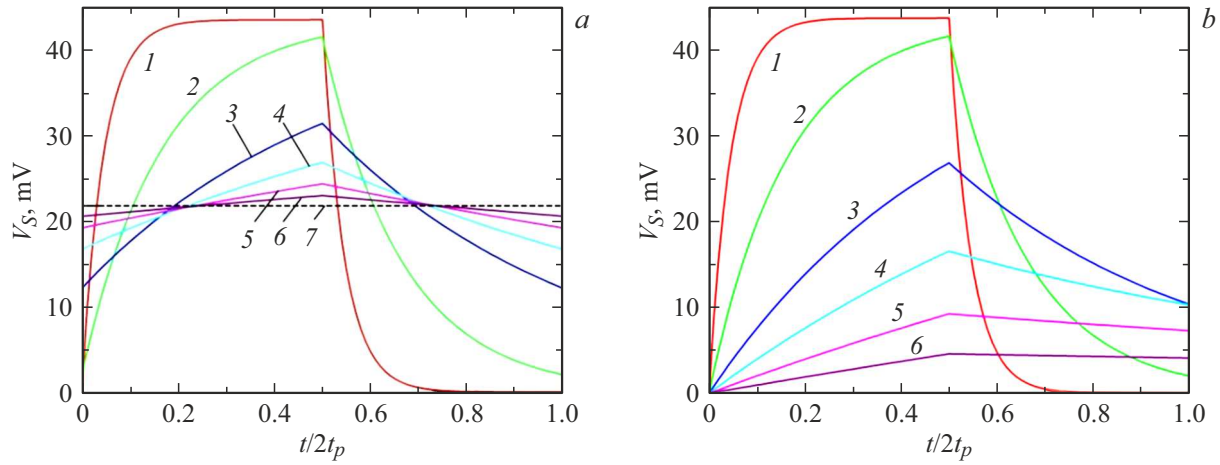

Figure 4. The theoretical dependence of the response of the bolometer V_S when exposed to rectangular pulses of THz radiation with a duration of $t_p = 1/2f$, with a period of $\Theta = 1/f = 2t_p$ (*a*) and with a period of $\Theta = 100/f = 200t_p$ (*b*). The dependences *1*–*6* correspond to frequencies f = 3, 11, 35, 70, 140, and 300 Hz; the straight line *7* corresponds to the mean value of V_S. Thermal relaxation time of the bolometer τ_0 = 15 ms.

of $t_p \gg \tau$. In consistency with the above, the signal value $V_{S,\mathrm{mean}} \approx 21$ mV, shown in Fig. 3, *b*, measured at frequency of $f = 3$ Hz, is close to half of the maximum signal $V_{S,\mathrm{max}} \approx 41$ mV shown in Fig. 1, *b*. The signal shape tends to a rectangular shape at low frequencies, i.e. when $t_p \gg \tau$, as can be seen from Fig. 4, and hence the RMS deviation $V_{S,\mathrm{rms}}$ tends to the value of $V_{S,P\mathrm{mean}}$. $\Delta V_S = V_S - V_{S,\mathrm{mean}}$ is proportional to the radiation pulse duration t_p at high frequencies (corresponding to the condition $t_p < \tau$), and the RMS deviation $V_{S,\mathrm{rms}}$ becomes inversely proportional to the pulse repetition rate. In general, the experimental data presented in Fig. 3, *b* correspond well to the theoretical dependencies calculated using the ratios given in Ref. [34] obtained within the framework of the bolometric model of signal formation.

The increase of the gas pressure in the vacuum housing of the MMDB results in an increase of the thermal conductivity G of the bolometer and a corresponding decrease of its thermal relaxation time τ. Fig. 5 shows the dependence of the mean value of the signal $V_{S,\mathrm{mean}}$ and its RMS deviation $V_{S,\mathrm{rms}}$ on the gas pressure P in the MMBD vacuum housing measured for different pulse repetition rates of the THz radiation. It can be seen that the average signal value $V_{S,\mathrm{mean}}$ virtually does not depend on the pressure at gas pressure less than 1 mbar, and it depends inversely on P at P more than 1 mbar: $V_{S,\mathrm{mean}} \propto 1/P$. In

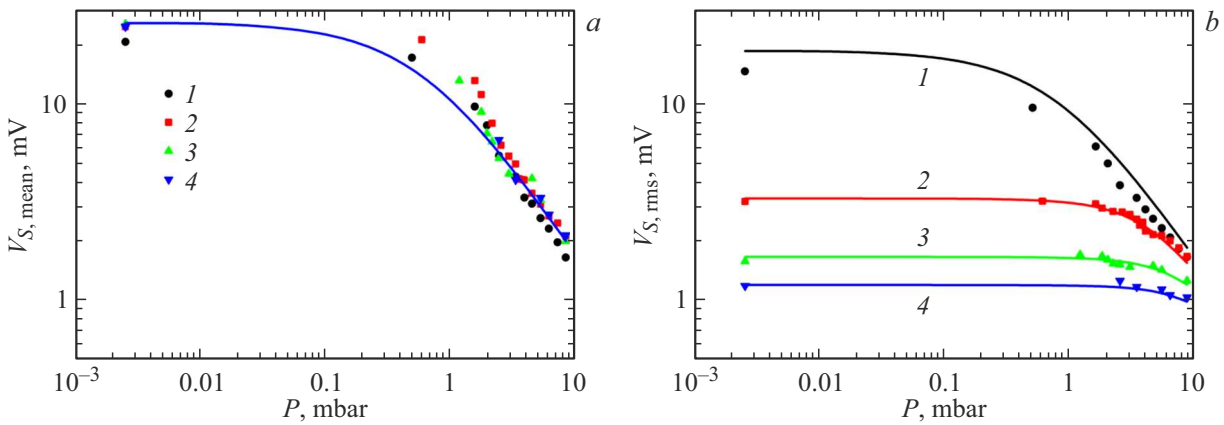

Figure 5. The dependences of the mean signal value $V_{S,\mathrm{mean}}$ (a) and its RMS deviation $V_{S,\mathrm{rms}}$ (b) on the gas pressure P in the MMBD vacuum housing, measured (points) and calculated (lines) at different values of THz radiation pulse repetition rates, f: *1* — 7, *2* — 40, *3* — 140, *4* — 195 Hz. Pulse ratio is 2.

accordance with the above, $V_{S,\mathrm{mean}}$ does not depend on the radiation pulse repetition rate. The RMS deviation of the signal $V_{S,\mathrm{rms}}$ at low frequencies has approximately the same dependence on the pressure as the mean value $V_{S,\mathrm{mean}}$, consistent with the fact that $V_{S,\mathrm{rms}} = V_{S,\mathrm{mean}}$ in the limiting case of $\Theta \gg \tau$ and a pulse ratio equal to two. At high frequencies $V_{S,\mathrm{rms}}$ weakly depends on the gas pressure and, hence, the thermal conductivity and the thermal relaxation time of the bolometer. Fig. 5 also shows the theoretical dependence calculated using the ratios given in Ref. [34] in which the dependence of the thermal conductivity of the bolometer G on the gas pressure P was defined by the following ratio [40]:

$$G = G_0 = \kappa_0 \frac{A}{d} \frac{1}{1 + CT_a/Pd}.$$

Here G_0 is the bolometer thermal conductivity under high vacuum; κ_0 — the specific thermal conductivity of air under normal conditions, equal to $28.4 \cdot 10^{-3}$ W/(K·m); A —the area of the microbolometer, equal to $1.6 \cdot 10^{-9}$ m^2; d — the thickness of the vacuum gap between the bolometer membrane and the substrate on which it is fabricated, equal to $2 \cdot 10^{-6}$ m; $C = 7.6 \cdot 10^{-5}$ N/(K·m) — a constant; $T_a = 300$ K — average absolute temperature of gas in the MMBD housing, P — gas pressure expressed in pascals.

For calculation of the dependences shown in Fig. 5, it was assumed that the pressure in the vacuum housing of the MMBD was 60% of the pressure measured by the sensor installed on the turbomolecular pump. It is clear that the experimental and calculated dependences coincide quite well. Given that the gas pressure of less than $P = 2.5 \cdot 10^{-3}$ mbar did not have any noticeable effect on the MMBD signal value, the experimental data corresponding to the pressure of $P = 2.5 \cdot 10^{-5}$ mbar, at which the turbomolecular vacuum pump was switched off, are moved to the point $P = 2.5 \cdot 10^{-3}$ mbar for clarity and compactness of Fig. 5. The pressure values changed too fast up to the value $P = 0.5$ mbar as the pump turbine decelerated, so experimental data are given either for pressures of $P \geq 0.5$ mbar, or for pressures at which the signal changes. The calculated dependences are given for the pressure range of $P = 2.5 \cdot 10^{-3}$ — 10 mbar.

3. The response of the microbolometer detectors to THz pulsed radiation with a large pulse ratio

We considered above the case when the radiation pulse ratio is 2, and the pulse repetition period Θ can be smaller than the bolometer thermal relaxation time τ. Next, we consider the case when the radiation pulse ratio is large, for example, equal to or greater than 10, and the radiation pulse repetition period is knowingly greater than τ. The bolometer has time to cool between two consecutive pulses in this case (Fig. 4, b). If the radiation pulse time t_p is much shorter than the bolometer relaxation time τ, then the value of the bolometer peak response V_s is proportional to the radiation pulse energy (or pulse duration t_p, if the radiation power does not change), not to its power, and it is inversely proportional to the bolometer heat capacity [34].

The QCL radiation was modulated by an external pulse voltage synchronized with the frame pulse controlling the MMDB operation in the following experimental studies of the dependences of the MMDB response on the THz-radiation pulse duration and on the gas pressure in the detector housing.

Since QCL and MMDB in this case were synchronized, by introducing a delay of the QCL pulse relative to the MMDB frame pulse we could read signals from the rows of the matrix detector, which were illuminated by THz radiation, either immediately after the end of the radiation pulse or just before its arrival (Fig. 6). It can be seen that during the time between radiation pulses, which is equal to $\Theta - t_p \approx 36-38$ ms, the microbolometers have time to cool down, because the bolometer thermal relaxation time

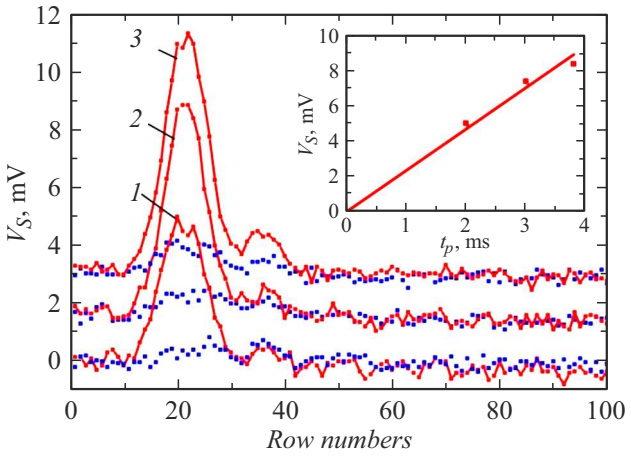

Figure 6. Distribution of the MMBD response V_S to a short pulse of THz radiation over the elements of the column of microbolometers passing through the maximum intensity of THz radiation. The frame rate and pulse repetition rate are 25 Hz, the duration of the radiation pulse: *1* — 2.0, *2* — 3.0, *3* — 3.8 ms. Lines with dots show signals measured immediately after the passage of the radiation pulse, points show signals measured just before its arrival. The inset shows the dependence of the response value V_s on the radiation pulse duration t_p. The pressure in the MMBD housing is $2.5 \cdot 10^{-5}$ mbar.

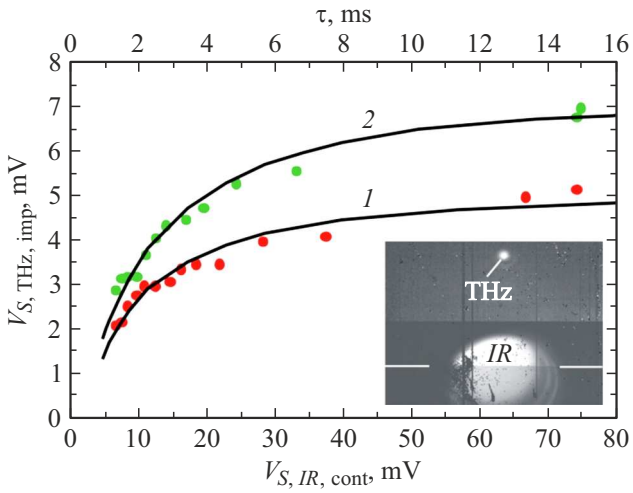

Figure 7. Experimental (dots) and theoretical (lines) dependences of the peak value of the MMBD signal $V_{S,\mathrm{THz,imp}}$ on the thermal relaxation time τ and the value of the signal in the region of constant IR illumination $V_{S,\mathrm{IR,\,cont}}$ when the MMBD is irradiated with THz radiation pulses with a duration of 2 (curve *1*) and 3 ms (curve *2*). The inset shows a topogram of the signals caused by constant IR and pulsed THz radiation.

$\tau_0 = 15$ ms is more than twofold less than the time between radiation pulses, and the magnitude of the MMBD response V_s is proportional to the duration of the radiation pulse t_p. It should be noted that the time of reading of signals from 20 lines on which the main peak of the signal is located is $(20/240)40\,\mathrm{ms} = 3.3\,\mathrm{ms}$, which is much less than τ_0 and, therefore, the measured spatial energy distribution of the THz radiation pulse is not significantly distorted because of the cooling of the microbolometers.

Both an image of an absolute black body (ABB) model heated to 400°C and an image of focused pulsed THz radiation were simultaneously created on the MMBD surface using lenses for studying the response of MMBD to short pulsed THz radiation depending on the thermal conductivity and the bolometer thermal relaxation time. The topogram of the observed signals is shown in the inset of Fig. 7. The upper and lower halves of the topogram were represented with different contrast because the signal from the THz-radiation QCL was much weaker than the signal from the ABB IR radiation. The regions corresponding to microbolometers with and without metal absorber are above and below the white horizontal dashes, respectively.

The constant IR radiation from a ABB was used to determine the thermal conductivity of the bolometer $G = G_0\ (V_{S,\mathrm{IR,cont_0}}/V_{S,\mathrm{IR,cont}})$ and, accordingly, the bolometer thermal relaxation time $\tau = \tau_0 G_0/G$, varying with the increase of the gas pressure in the MMBD housing. Here $V_{S,\mathrm{IR,cont_0}}$ and $V_{S,\mathrm{IR,cont}}$ — the values of the signal in a region of constant IR illumination with high and low vacuum, respectively. Fig. 7 shows the dependence of the peak value of the MMBD signal $V_{S,\mathrm{THz,\,imp}}$ on the thermal relaxation time τ in case of irradiation with short pulses of THz radiation (period $\Theta = 40$ ms). Theoretical dependences were calculated using the ratios given in Ref. [34]. It is apparent that there is good agreement between the experiment and theory. In particular, the value of signal $V_{S,\mathrm{THz,\,imp}}$ weakly depends on τ at values τ much larger than the radiation pulse duration t_p in agreement with what is stated in Ref. [34].

The inset in Fig. 7 shows that the presence of a metal absorber increases the bolometer signal not only in the case of THz radiation, but in the case of infrared radiation ABB (the signal level from the ABB is higher in the region, consisting of a microbolometer with a thin metal absorber — the signal increases from dark to light in the topographic image). However, it should be noted that in the case of QCL narrowband radiation the increase of the magnitude of the signal $V_{S,\mathrm{THz,\,imp}}$ means higher volt-watt sensitivity to the THz radiation, while in the case of broadband infrared radiation of ABB the signal increases due to the widening of the absorption bands. Indeed, IR radiation is absorbed by the silicon oxynitride membrane of the microbolometer in a rather narrow wavelength range ($8-13.5\,\mu$m [41]) in the absence of a thin metal absorber, and in the presence of a metal absorber it is absorbed in a wider range (for example, $6-50\,\mu$m with the layer resistance of the absorber equal to $100\,\Omega/\square$ [42]), limited by wave interference in a thin resonator formed by a metal absorber and a mirror deposited on a silicon substrate located at a distance $\approx 2.5\,\mu$m from the bolometer membrane. In this case the volt-watt sensitivity to IR

radiation in the range of $8-14\,\mu$m may even be reduced by the presence of a metal absorber [5].

Minimum detectable energy of the THz radiation pulse Q_{th} can be determined by the peak value of the signal $V_{S,\mathrm{THz,\,imp}} = 7\,$mV, measured at the center of the focused THz radiation with a pulse duration of $t_p = 3\,$ms (Fig. 6), and incident on the corresponding pixel of the radiation power $P_{\mathrm{pix,max}} \approx 2.3 \cdot 10^{-7}\,$W found in sect. 2. The value $Q_{th} = P_{\mathrm{pix,max}} t_p \ (V_{\mathrm{noise}}/V_{S,\mathrm{THz,\,imp}}) \approx 2.5 \cdot 10^{-11}\,$J obtained using this method is close to the value that can be obtained by another method: $Q_{th} = \tau_0 P_{th} = 2.1 \cdot 10^{-11}\,$J, where P_{th} — the minimum detectable power equal to $1.4 \cdot 10^{-9}\,$W found in Sec. 2. It should be noted that the reduction of P_{th} (approximately 20 times) achieved in this study in comparison with similar detectors presented in Ref. [6], is attributable, first, to the replacement of the sol-gel method of obtaining the thermosensitive vanadium oxide layer by a more advanced ion-beam technology, secondly, to the use of thin metallic absorbers of THz radiation, thirdly, to the replacement of germanium input window with silicon one, and fourthly, to the increase of bolometer bias voltage from 1 to 1. 5 V, which accordingly resulted in the reduction of P_{th} by 2, 2, 3, and 1.5 times (total $2 \times 2 \times 3 \times 1.5 = 18$). In addition, the value P_{th} given in this paper was obtained for the wavelength of THz radiation equal to $100\,\mu$m, while it was obtained in Ref. [6] for a wavelength equal to $130\,\mu$m, which also contributes to a decrease of P_{th} because of an increase of the radiation absorption coefficient (see Fig. 11 in Ref. [37]). The latter is attributable to the fact that in the case of wavelengths λ well above the suspension height of the microbolometer membrane h, the thin metal radiation absorber is near the standing wave node formed by the reflection of the incident radiation from the metal reflector located below the bolometer on the surface of the silicon readout circuit. In this case, the electric field in the absorber region and, consequently, the value of the absorption coefficient appear small but they increase proportionally to h/λ with the decrease of the wavelength, reaching a maximum under the well-known condition $h = \lambda/4$ [7].

Further increase of the sensitivity of microbolometers with a thin metal absorber to THz radiation can be achieved by use of input silicon window with an anti-reflective coating, increasing the suspension height of the microbolometer membrane with an absorber applied to it, reduction of heat capacity (when detecting short pulses of radiation) and thermal conductivity of microbolometers (when detecting long pulses or constant radiation).

Conclusion

It was found that the dependences of the MMBD response on the duration of the THz radiation pulse, its repetition rate, gas pressure in the detector housing, thermal conductivity, and the value of the bolometer thermal relaxation time are well described by the theoretical ratios obtained in the framework of the bolometric model [34], which makes it possible to confidently use these detectors for monitoring and measuring the parameters of pulsed THz radiation under various conditions.

It was shown that the signal of a microbolometer detector exposed to pulsed THz radiation weakly depends on the thermal conductivity of the bolometer and, accordingly, on the thermal relaxation time of the bolometer, if the duration of radiation pulses is less than the thermal relaxation time of the bolometer. This makes it possible to produce highly sensitive pulsed radiation detectors operating at a frame frequency of several hundred Hertz. The detectors studied at the wavelength of $100\,\mu$m have a minimum detectable power of $1.4 \cdot 10^{-9}\,$W and the minimum detectable energy of $2.5 \cdot 10^{-11}\,$J, while demonstrating high sensitivity to the direction of polarization of THz radiation.

Funding

This study was carried out under state assignment FWGW-2022-0007.

Conflict of interest

The authors declare that they have no conflict of interest.

References

[1] A. Rogalski. Progr. Quant. Electron., **27** (2–3), 59 (2003). DOI: 10.1016/S0079-6727(02)00024-1
[2] A. Rogalski. Progr. Quant. Electron., **36** (2–3), 342 (2012). DOI: 10.1016/j.pquantelec.2012.07.001
[3] A. Rogalski. Opto–Electron. Rev., **21** (4), 406 (2013). DOI: 10.2478/s11772-013-0110-x
[4] A.W.M. Lee, B.S. Williams, S. Kumar, Q. Hu, J.L. Reno. IEEE Photon. Technol. Lett., **18** (13), 1415 (2006). DOI: 10.1109/LPT.2006.877220
[5] N. Oda. C.R. Physiq., **11** (7–8), 496 (2010). DOI: 10.1016/j.crhy.2010.05.001
[6] M.A. Dem'yanenko, D.G. Esaev, B.A. Knyazev, G.N. Kulipanov, N.A. Vinokurov. Appl. Phys. Lett., **92** (13), 131116 (2008). DOI: 10.1063/1.2898138
[7] N. Nemoto, N. Kanda, R. Imai, K. Konishi, M. Miyoshi, S. Kurashina, T. Sasaki, N. Oda, M. Kuwata-Gonokami. IEEE Trans. Terahertz Sci. Technol., **6** (2), 175 (2016). DOI: 10.1109/TTHZ.2015.2508010
[8] F. Simoens, J. Meilhan. Philosophical Transactions Royal Society of London A: Mathematical, Physical and Engineering Sciences, **372** (2012), 20130111 (2014). DOI: 10.1098/rsta.2013.0111
[9] F. Simoens, J. Meilhan, J.-A. Nicolas. J. Infrared Milli Terahz Waves, **36** (10), 961 (2015). DOI: 10.1007/s10762-015-0197-x
[10] Y. Amarasinghe, W. Zhang, R. Zhang, D.M. Mittleman, J. Ma. J. Infrared, Millimeter, Terahertz Waves, **41** (2), 215 (2020). DOI: 10.1007/s10762-019-00647-4
[11] Y. Yang, A. Shutler, D. Grischkowsky. Opt. Express, **19** (9), 8830 (2011). DOI: 10.1364/OE.19.008830

[12] G.S. Kent, B.R. Clemesha, R.W. Wright. J. Atmospheric Terrestrial Phys., **29** (2), 169 (1967). DOI: 10.1016/0021-9169(67)90131-6
[13] G.S. Kent, R.W. Wright. J. Atmospheric Terrestrial Phys., **32** (5), 917 (1970). DOI: 10.1016/0021-9169(70)90036-X
[14] G.-R. Kim, T.-I. Jeon, D. Grischkowsky. Opt. Express, **25** (21), 25422 (2017). DOI: 10.1364/OE.25.025422
[15] Y. Yang, M. Mandehgar, D. Grischkowsky. Opt. Express, **20** (24), 26208 (2012). DOI: 10.1364/OE.20.026208
[16] J.M. Dai, X.F. Lu, J. Liu, I.C. Ho, N. Karpowicz, X.-C. Zhang. Terahertz Sci. Technol., **2** (4), 131 (2009). DOI: 10.11906/TST.131-143.2009.12.14
[17] L.-Z. Tang, J.-Y. Zhao, Z.-H. Dong, Z.-H. Liu, W.-T. Xiong, Y.-C. Hui, A. Shkurinov, Y. Peng, Y.-M. Zhu. Opt. Laser Technol., **141**, 107102 (2021). DOI: 10.1016/j.optlastec.2021.107102
[18] G.-R. Kim, K. Moon, K.H. Park, J.F. O'Hara, D. Grischkowsky, T.-I. Jeon. Opt. Express, **27** (20), 27514 (2019). DOI: 10.1364/OE.27.027514
[19] D.S. Sitnikov, S.A. Romashevskiy, A.A. Pronkin, I.V. Ilina. J. Physics: Conf. Ser., **1147**, 012061 (2019). DOI: 10.1088/1742-6596/1147/1/012061
[20] V.L. Granatsteina, G.S. Nusinovich. J. Appl. Phys., **108** (6), 063304 (2010). DOI: 10.1063/1.3484044
[21] G.S. Nusinovich, D.G. Kashyn, Y. Tatematsu, T. Idehara. Phys. Plasmas, **21** (1), 013108 (2014). DOI: 10.1063/1.4862779
[22] C.W. Berry, M.R. Hashemi, M. Jarrahi. Appl. Phys. Lett., **104** (8), 081122 (2014). DOI: 10.1063/1.4866807
[23] D.S. Kim, D.S. Citrin. Appl. Phys. Lett., **88** (16), 161117 (2006). DOI: 10.1063/1.2196480
[24] H. Hirori, A. Doi, F. Blanchard, K. Tanaka. Appl. Phys. Lett., **98** (8), 091106 (2011). DOI: 10.1063/1.3560062
[25] M.A. Belkin, F. Capasso. Phys. Scripta, **90** (11), 118002 (2015). DOI: 10.1088/0031-8949/90/11/118002
[26] L. Li, L. Chen, J. Zhu, J. Freeman, P. Dean, A. Valavanis, A.G. Davies, E.H. Linfield. Electron. Lett., **50** (4), 309 (2014). DOI: 10.1049/el.2013.4035
[27] Q. Lu, M. Razeghi. Photonics, **3** (3), 42 (2016). DOI: 10.3390/photonics3030042
[28] G. Liao, Y. Li, H. Liu, G.G. Scott, D. Neely, Y. Zhang, B. Zhu, Z. Zhang, C. Armstrong, E. Zemaityte, P. Bradford, P.G. Huggard, D.R. Rusby, P. McKenna, C.M. Brenner, N.C. Woolsey, W. Wang, Z. Sheng, J. Zhang. Proc. National. Acad. Sci. USA, **116** (10), 3994 (2019). DOI: 10.1073/pnas.1815256116
[29] X. Wu, D. Kong, S. Hao, Y. Zeng, X. Yu, B. Zhang, M. Dai, S. Liu, J. Wang, Z. Ren, S. Chen, J. Sang, K. Wang, D. Zhang, Z. Liu, J. Gui, X. Yang, Y. Xu, Y. Leng, Y. Li, L. Song, Y. Tian, R. Li. Adv. Mater., **35** (23), 2208947 (2023). DOI: 10.1002/adma.202208947
[30] B. Zhang, Z. Ma, J. Ma, X. Wu, C. Ouyang, D. Kong, T. Hong, X. Wang, P. Yang, L. Chen, Y. Li, J. Zhang. Laser Photon. Rev., **15** (3), 2000295 (2021). DOI: 10.1002/lpor.202000295
[31] Z. Yu, N. Zhang, J. Wang, Z. Dai, C. Gong, L. Lin, L. Guo, W. Liu. Opto-Electron. Adv., **5** (9), 210065 (2022). DOI: 10.29026/oea.2022.210065
[32] V.L. Bratman, A.A. Bogdashov, G.G. Denisov, M.Yu. Glyavin, Yu.K. Kalynov, A.G. Luchinin, V.N. Manuilov, V.E. Zapevalov, N.A. Zavolsky, V.G. Zorin. J. Infrared Milli Terahz Waves, **33** (7), 715 (2012). DOI: 10.1007/s10762-012-9898-6
[33] G.S. Nusinovich, R. Pu, T.M. Antonsen Jr., O.V. Sinitsyn, J. Rodgers, A. Mohamed, J. Silverman, M. Al-Sheikhly, Y.S. Dimant, G.M. Milikh, M.Yu. Glyavin, A.G. Luchinin, E.A. Kopelovich, V.L. Granatstein. J. Infrared Milli Terahz Waves, **32** (3), 380 (2011). DOI: 10.1007/s10762-010-9708-y
[34] M.A. Dem'yanenko, V.V. Startsev. Tech. Phys., **67** (3), 347 (2022). DOI: 10.21883/TP.2022.03.53266.190-21
[35] V.Sh. Aliev, M.A. Dem'yanenko, D.G. Esaev, I.V. Marchishin, V.N. Ovsyuk, B.I. Fomin. Uspekhi prikladnoi fiziki, **1** (4), 471 (2013) (in Russian).
[36] M.A. Dem'yanenko, B.I. Fomin, L.L. Vasilieva, S.A. Volkov, I.V. Marchishin, D.G. Esaev, V.N. Ovsyuk, V.L. Dshkhunyan, E.B. Volodin, A.V. Ermolov, P.P. Usov, V.P. Chesnokov, Yu.S. Chetverov, P.N. Kudryavtsev, A.E. Zdobnikov, A.A. Ignatov. Prikladnaya fizika, **4**, 124 (2010). (in Russian).
[37] N. Oda, H. Yoneyama, T. Sasaki, M. Sanoa, S. Kurashina, I. Hosako, N. Sekine, T. Sudoh, T. Irie. Proc. SPIE, **6940**, 69402Y (2008). DOI: 10.1117/12.781630
[38] A.J.L. Adam, I. Kašalynas, J.N. Hovenier, T.O. Klaassen, J.R. Gao, E.E. Orlova, B.S. Williams, S. Kumar, Q. Hu, J.L. Reno. Appl. Phys. Lett., **88** (15), 151105 (2006). DOI: 10.1063/1.2194889
[39] E.E. Orlova, J.N. Hovenier, T.O. Klaassen, I. Kašalynas, A.J.L. Adam, J.R. Gao, T.M. Klapwijk, B.S. Williams, S. Kumar, Q. Hu, J.L. Reno. Phys. Rev. Lett., **96** (17), 173904 (2006). DOI: 10.1103/PhysRevLett.96.173904
[40] H. Wu, S. Grabarnik, A. Emadi, G. de Graaf, R.F. Wolffenbuttel. J. Micromech. Microeng., **19** (7), 074022 (2009). DOI: 10.1088/0960-1317/19/7/074022
[41] J. Dupuis, E. Fourmond, D. Ballutaud, N. Bererd, M. Lemiti. Thin Solid Films, **519** (4), 1325 (2010). DOI: 10.1016/j.tsf.2010.09.036
[42] M.A. Dem'yanenko. J. Opt. Technol., **84** (1), 34 (2017). DOI: 10.1364/JOT.84.000034

Translated by A.Akhtyamov